# Droplet Bouncing on Cold Wall: Comparison of Experiments with Direct Numerical Simulations

N. Roth*, H. Gomaa, N. Bordoni, T. Dumont and B. Weigand
Institute of Aerospace Thermodynamics
Universität Stuttgart
Pfaffenwaldring 31
70569 Stuttgart

**Abstract**

Bouncing of ethanol droplets on a smooth glass wall have been investigated experimentally and numerically using the same initial and boundary conditions. The results of the experiments and the numerical simulations show very good agreement. The topology of the droplets as well as the spacing between wall and droplet liquid have been compared. Thus, the detailed results of the numerical simulations can be used to obtain a better understanding of the physical processes during the impact of droplets on a solid wall.

---

## Introduction

The impact of droplets on solid surfaces plays an important role in many natural and technical systems as e.g. when raindrops fall on earth or droplets impinge on the walls of a combustion chamber. In order to understand and/or to improve these systems a physical understanding of the detailed droplet dynamic processes is necessary. The processes may be studied analytically, experimentally or numerically. Each of these methods has its own well known advantages and disadvantages. The most comprehensive understanding of droplet dynamic processes may be possible in a combination of all or parts of these methods.

The most detailed information is obtained by Direct Numerical Simulations (DNS). However, the DNS may lasten too long in comparison with calculations using analytical solutions or the problem may be too large for the available computer systems. If this is not the case DNS provides a comprehensive information about the droplet process, however, it has to be taken into account, that numerical simulations need in any case a validation.

In this paper we present an experimental validation of numerical simulations of the bouncing process of droplets on smooth dry walls at room temperature. Simulations of such a bouncing process have been reported in [1] in detail. Here, results of simulations are compared with corresponding experiments.

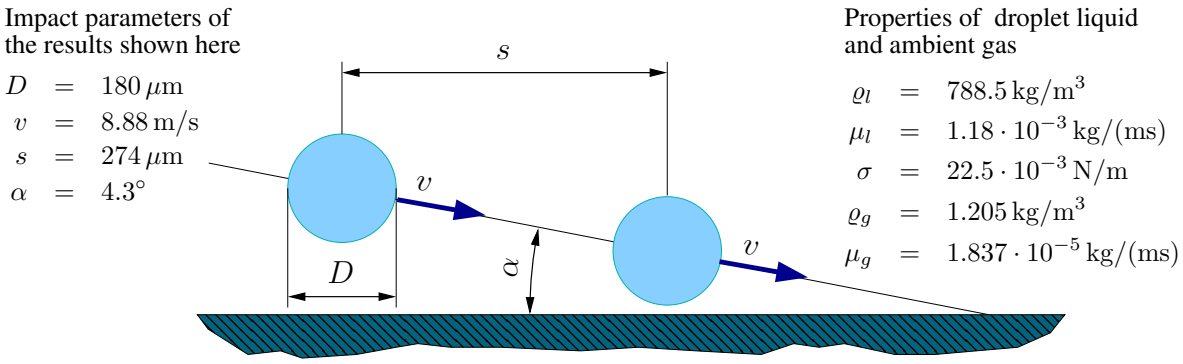


**Figure 1.** Schematical drawing for the definition of the impact parameters. Besides the impact angle $\alpha$, the diameter $D$, the velocity $v$ and the spacing $s$ of the droplet, the properties of the droplet liquid (here ethanol) as density $\varrho_l$, viscosity $\mu_l$, surface tension $\sigma$ with respect to the ambient gas and the properties of the surrounding gas as density $\varrho_g$, viscosity $\mu_g$ are important for the bouncing process.

The system which is studied numerically and experimentally is schematically depicted in Fig. 1. There, the parameters characterizing the impact of a monodisperse droplet stream on a solid wall are shown and specified, which are relevant for this paper. In the next section the experimental and numerical methods used for the comparison are described.

*Corresponding author: norbert.roth@itlr.uni-stuttgart.de

## Materials and Methods

### *Experimental Method*

In the experiments a monodisperse droplet stream is used, which impacts on a glass surface. The droplet stream is produced using a droplet stream generator, described e.g. in [2]. The droplets in the stream have all the same size, velocity and temperature at the moment, when they impact on the surface, which is in this case a right-angled and equal-sided glass prism as shown schematically in Fig. 2. The impact process is observed with

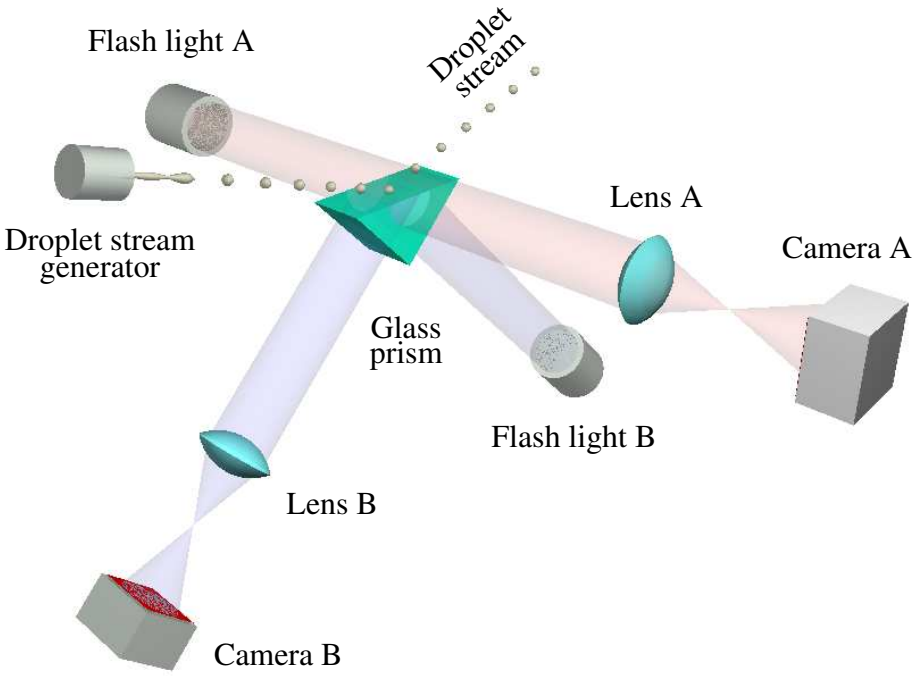


**Figure 2.** Schematical view of the experimental setup. Shown are the lightpaths of both observation methods.

two different methods depicted in Fig. 2. Shodowgraphs of the droplet impact are taken by camera A, with flash light A as light source and lens A as objective. The flash light has a very short duration in order to freeze the droplet motion. The direction of observation is not exactly horizontal, the camera A looks on the glass surface at a very small angle in order to obtain sharp images of the droplets, which are not disturbed by the edge of the glass prism. With the second observation method one obtains information about the spacing between the glass surface and the droplet liquid during the bouncing process. The light of flash light B is totally internally reflected at the glass surface, where the droplets impact on, as shown in Fig. 2. This light is detected by camera B. The lens B images the surface at the place of the impact. At the glass surface evanescent waves develop above the surface during the total internal reflection. During the bouncing process the droplet liquid does not wet, but approaches the glass surface very closely. There, evanescent waves are disturbed and not all light is totally reflected and reaches camera B. At the locations, where the droplet liquid is closer, more light of the evanescent waves is disturbed and there the images of camera B become darker. Therefore the images of camera B are at least a qualitative measure of the spacing between the glass surface and the droplet liquid. A detailed description of this observation method is given in [3]. The experimental method allows to measure and control the initial and boundary conditions very precisely, which is absolutely necessary for comparisons with numerical simulations.

### *Numerical Method*

For the Direct Numerical Simulations (DNS) the code FS3D, developed at the ITLR has been used, which is described in detail in [4]. The code FS3D solves the incompressible 3D Navier-Stokes equations. In order to describe free liquid surfaces the Volume-Of-Fluid (VOF) method is used. Simulations of the droplet impact on cold walls have already been reported in detail in [1], however without any validation.

In order to facilitate the understanding of results of the DNS the numerical setup, the boundary and initial conditions are described in the following. In the simulations the same conditions have been used as in corresponding experimental studies. Only cases with no wetting of the wall and without any heat transfer processes have been studied. Therefore the properties of the wall itself have not to be taken into account. The energy equation has not

been solved. The temperature of the ambient air, the droplet, and the wall was constant at $T_0 = 293.15\,\mathrm{K}$. The properties of the droplet liquid and the ambient air are given in Fig. 1.

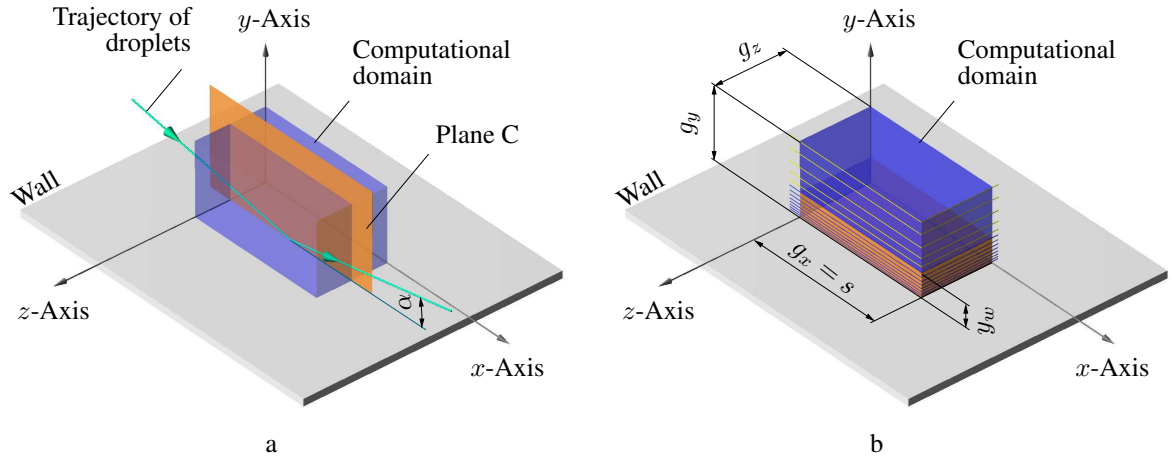


**Figure 3.** On the left hand side (a): schematic view of the geometric arrangement used for the simulations including the computational domain, the trajectory of the droplets and the impact angle $\alpha$. On the right hand side (b): sketch indicating the size of the computational domain and the grid refinement in $y$-direction near the wall. The position of every $n$th layer of grid cells in the $x, z$-plane is marked.

The geometric arrangement for the simulations is shown schematically in Fig. 3 a. The plane C can be defined by the trajectory of the incoming droplets and by the trajectory of the reflected droplets. This plane is naturally perpendicular to the wall. The intersection of this plane with the wall defines the $x$-direction. The $z$-direction is perpendicular to plane C and the $y$-direction is perpendicular to the wall. The bottom of the computational domain is the wall. The origin of the $x, y, z$-axes is in one corner of the block-shaped computational domain, the edges of the computational domain are oriented along the $x$-,$y$- and $z$-axis, respectively, as can be seen from Fig. 3 a. Plane C cuts the computational domain into halves. The width of the computational domain in $x$-direction $g_x = s$ equals the horizontal spacing of the droplets in the experiments. The width in $y$-direction (height) and $z$-direction (depth) $g_y = g_z = 300\,\mu\mathrm{m}$ for all calculations shown here. The boundary conditions have been set as follows for all simulations. At the bottom of the computational domain, no slip conditions have been applied. For the other three sides of the computational domain, which are parallel to the $x$-direction von Neumann boundary conditions are used. It should be emphasized, that attention has been payed to the fact, that during the boucing process no liquid mass passes these three boundaries. For the remaining sides perpendicular to the $x$-direction periodic boundary conditions have been used. As a result liquid mass leaving the computational domain at $x = g_x$ will immediately enter the computational domain at $x = 0$. This can be interpreted as the simulation of a monodisperse droplet stream impact on the wall or glass surface respectively. The simulations have been performed fully 3D without any symmetry assumptions. A rectangular grid has been used with refinements near the wall. In $x$-direction and in $z$-direction the size $\Delta x$ or $\Delta z$ (width or depth) of the grid cells is equidistant in each case and can easily be calculated from the size of the computational domain and the number of grid cells $n_x = 256$ or $n_z = 128$, respectively. As mentioned above the vertical size of the grid cells becomes smaller near the wall. The computational domain is divided in $y$-direction in two sections: a lower section for $0 \leq y \leq y_w = 100\,\mu\mathrm{m}$ with $n_{yl} = 80$ grid cells and an upper section for $y_w \leq y \leq g_y$ with $n_{yu} = 48$ grid cells. The total number of grid cells in $y$-direction is $n_y = n_{yl} + n_{yu} = 128$, as illustrated in Fig. 3 b by indicating both sections and in addition each $n$th position of grid cells in $y$-direction. The plane with the smallest grid cells is located directly at the wall with the height $\Delta y(1) = 0.3125\,\mu\mathrm{m}$. For increasing $y$-values the height of the grid cells increases. The difference in height between neighbouring grid cells is constant, however, this constant value differs between the lower and upper section. In the upper section the smallest height of the grid cells at $y(n_{yl} + 1)$ equals the height of the grid cells at $y(n_{yl})$.

**Results and Discussion**

With the experimental and numerical setups described above several experiments and DNS have been performed. In this section one example is presented. The impact parameters have been depicted already in Fig. 1

together with the properties of the droplet liquid ethanol and the properties of the ambient gas (air).

***Experimental Results***

Experimental images from both cameras A and B are depicted in Fig. 2. Figure 4A taken with camera A shows the impact and bouncing of the droplet stream. In the center of the droplets a bright spot can be observed, which is caused by rays passing the droplet and being focussed shortly behind the droplets. A mirror image of each droplet

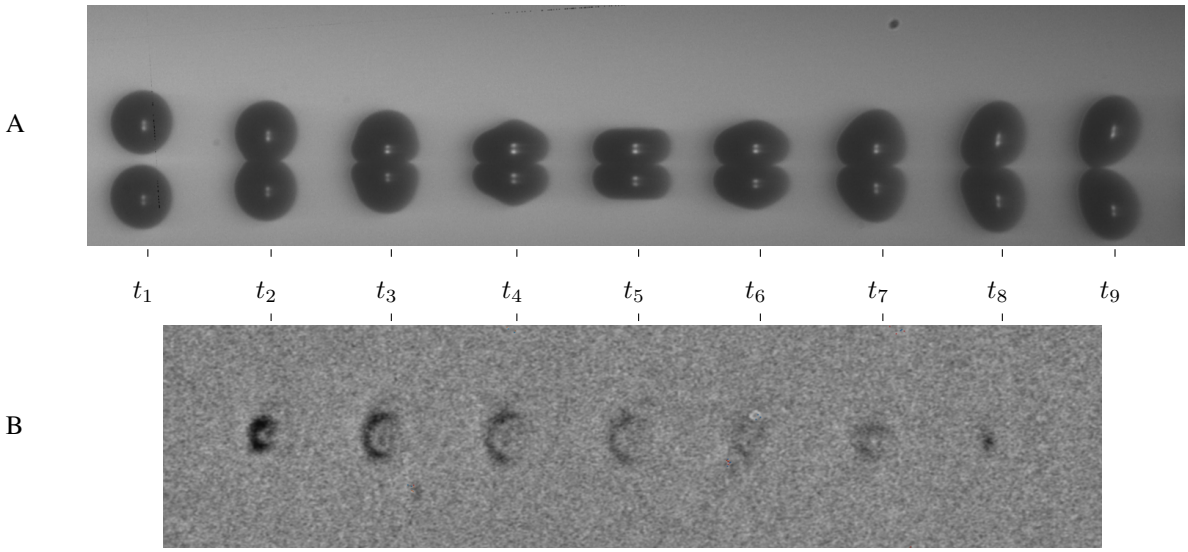


**Figure 4.** At the top (A): shadowgraph of the impact of the droplet stream taken by camera A, at the bottom (B): disturbed totally internally reflected light taken by camera B characterizing the spacing between glass surface and droplet liquid.

can be seen on the glass surface. Each droplet of the droplet stream shows the state of the bouncing process at one moment $t_i$. In order to determine the impact parameters as impact angle $\alpha$, droplet size $D$, velocity $v$, and spacing $s$ such pictures are used. A picture of the disturbed totally internally reflected light taken by camera B is depicted in Fig. 4B. The closer the droplet liquid approaches the glass surface, the more the light is disturbed and the darker becomes the picture characterizing at least qualitatively the spacing between glass surface and the droplet liquid. As both flash lights A and B are triggered at the same time each dark region of the totally internally reflected light can be related to a droplet. The experimental results can directly be compared with the results obtained by DNS.

***Numerical Results***

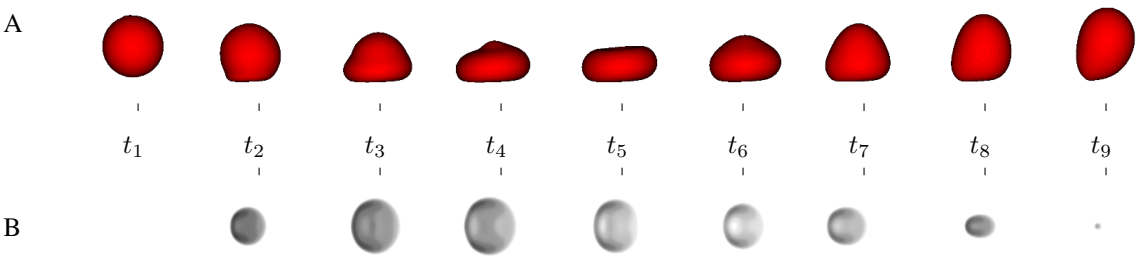


**Figure 5.** At the top (A) results of a DNS of the bouncing process at different times $t_i$ corresponding to the states of the bouncing process shown in Fig. 4. Like in the experiments the view is not exactly horizontal. At the bottom (B) corresponding calculations to the images at the top of the spacing between wall and droplet liquid. The gray levels indicate the spacing linearly with spacing zero as black and spacing $3\,\mu\mathrm{m}$ as white.

The results shown in Fig. 5 correspond to the experimental results shown above. The impact parameters and the

boundary conditions are the same. In order to take account for the droplet stream the length of the computational region $g_x = s = 274\,\mu\mathrm{m}$ is the same as the horizontal droplet distance in the experiment depicted above. The topologies of the droplets obtained by the DNS are shown in Fig. 5A at the same times $t_i$ of the bouncing process. In Fig. 5B calculations of the spacing between droplet liquid and wall characterized by different gray levels are shown for the same times $t_i$.

***Comparisons***

In this section comparisons between the experimental and numerical results, which are shown above, are presented. For the comparison of the topology overlays between images of droplets in the droplet stream and corresponding images derived from numerical simulations are performed, as shown in Fig. 6. After some corrections the topology of the experiments can be compared with the numerically optained topology. From Fig. 7, where the

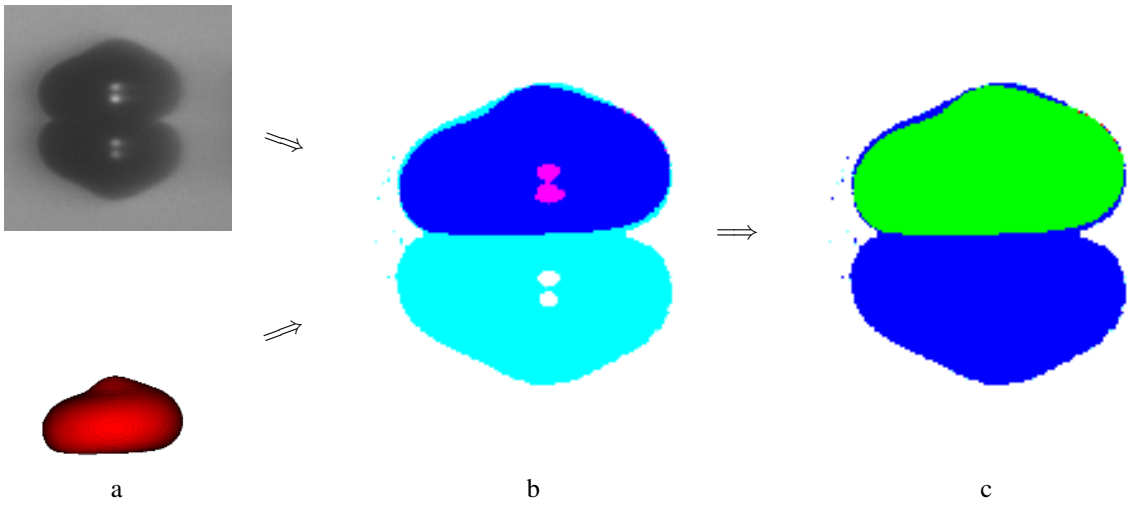


**Figure 6.** Topological comparison between experiment and DNS at $t = t_4$. From images of camera A and corresponding DNS (a) overlays are produced (b), which are modified with respect to the bright spot in the images and the color table (c). The common shape is depicted in green, deviations of the experiments are in blue (the mirrored droplet is no deviation) and deviations of the DNS are in red.

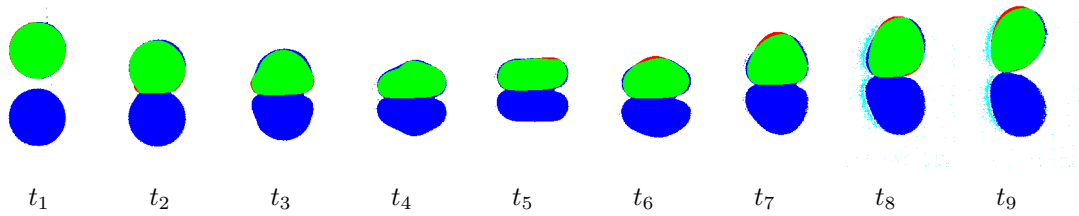


**Figure 7.** Topological comparison between experiment and DNS for different times $t_i$ of the bouncing process.

comparisons for the total droplet stream is shown, the very good agreement of the droplet topology between the experiment and the DNS can be seen. However, not only the topology of the droplets can be compared, in addition the spacing between droplet liquid and the wall can be compared qualitatively. The process how to compare the experimental results that means the totally internally reflected light with numerical calculations is described in Fig. 8. For all droplets in the droplet stream the comparison is shown in Fig. 9. Even for the very sensitve spacing between droplet liquid and wall good agreement between experiment and DNS can be observed.

**Conclusion**

Experiments using monodisperse droplet streams and Direct Numerical Simulations (DNS) using the inhouse code FS3D have been performed for the same initial and boundary conditions. The experimental techniquew allow

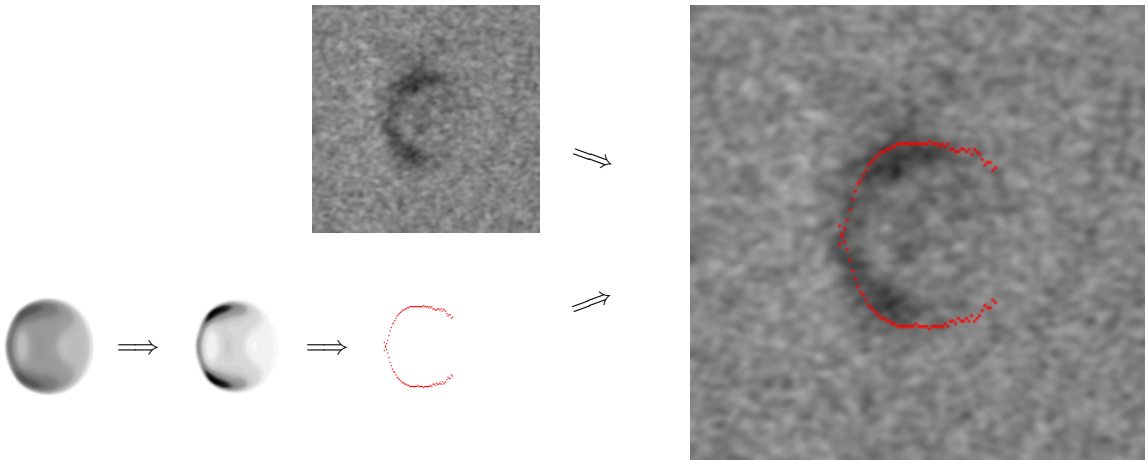


**Figure 8.** Numerically calculated spacing between droplet liquid and wall in linear scale at $t = t_4$ (a) and the same in nonlinear scale according to the decay of the intensity of the evanescent waves (b). Under (c) at top image of the totally internally reflected light for $t = t_4$ and at the bottom a line giving the smallest spacings derived from the calculation shown under (b). For comparison under (d) an overlay of the images shown under (c).

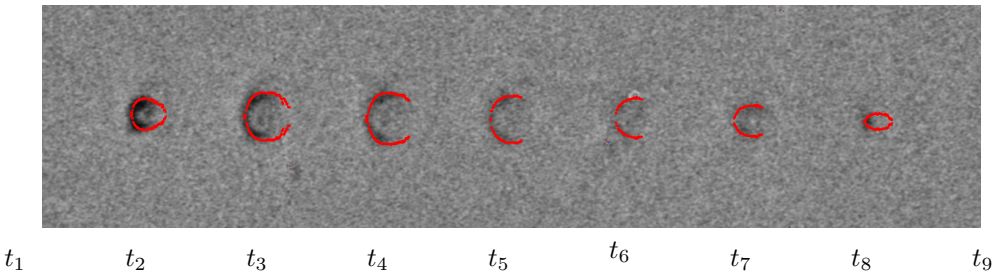


**Figure 9.** Overlays as described in Fig. 8d for different times $t_i$ comparing corresponding experimental and numerical results.

to adjust and measure all important impact parameters and boundary conditions. This is the basis for detailed comparisons with numerical simulations. This comparisons show very good agreement. Therefore the very comprehensive information of the bouncing process obtained by numerical simulations can be relied on. This, however, is necessary to improve the physical understanding of this process.

## References

[1] N. Roth, J. Schlottke, J. Urban, and B. Weigand. Simulations of droplet impact on cold wall without wetting. In *Proc. 22th Int. Conf. on Liquid Atomization and Spray Systems*, pp. 9–1, Como, 2008. ILASS.

[2] A. Frohn and N. Roth. *Dynamics of Droplets*. Experimental Fluid Mechanics. Springer-Verlag, Berlin, 2000.

[3] N. Roth, T. Straub, and B. Weigand. Observation method to obtain information on the vapour film during the collision of droplets with hot walls. In *Proc. 9th Int. Conf. on Liquid Atomization and Spray Systems*, pp. 0807. ICLASS, 2003.

[4] J. Schlottke and B. Weigand. Direct numerical simulation of evaporating droplets. *Journal of Computational Physics*, Vol. 227, pp. 5215–5237, 2008.